16th CIRP Conference on Modelling of Machining Operations

A new methodology for evaluation of mechanical properties of materials at very high rates of loading

Tiago dos Santos[a,b], José Carlos Outeiro[c], Rodrigo Rossi[a], Pedro Rosa[d,*]

[a]Departamento de Engenharia Mecânica, Univ. Federal do Rio Grande do Sul, Rua Sarmento Leite, 425, Porto Alegre, RS, 90046-902, Brazil.

[b]CAPES Foundation, Ministry of Education of Brazil, Brasília, DF, 70040-020, Brazil

[c]aLaBoMaP, Arts et Metiers ParisTech 71250, Cluny, France

[d]IDMEC, Instituto Superior Técnico, Universidade de Lisboa, Av. Rovisco Pais N1, 1049-001, Lisboa, Portugal

* Corresponding author. Tel.: +351-21-841-7213. E-mail address: pedro.rosa@tecnico.ulisboa.pt

Abstract

This paper focuses on the development of a straight forward and inexpensive testing machine, and methodology for the characterization of materials in working conditions similar to those found in metal cutting. Special emphasis is given to the material rate dependence and to the assessing of the proposed methodology against conventional testing at very high rates of loading. The experimental results have demonstrated that rate-dependent hardness can be used to estimate flow stress at high rates of loading and that contact phenomena become even more prominent for severe monotonic deformation.

Keywords: Mechanical characterization; Testing machine, Experimental methodology, Flow stress, Material hardness, High strain rate effect; AA1050.

1. Main text

Flow stress is among the most determining input data for the numerical simulation of metal cutting. This instantaneous material response is governed by a complicated interaction of several factors such as microstructural evolution, deformation-history and temperature. There are many constitutive models that can be used to deal with material response modelling; some physically-based models have been proposed to correlate metallurgical or physical aspects with corresponding constitutive description [1]. However, this class of constitutive proposals demands a large number of experimental tests, requires complex optimization algorithms and large computational efforts to find associated model constants, and not always have an adequate outcome [2]. Therefore, material is assumed to be both continuous and isotropic, and less intricate semi-physical constitutive models, also known as phenomenological [3], as well empirical equations are used

under the explanation of its simple form and good prediction characteristics. This is probably the reason why most of works in the literature have adopted the empirical Johnson–Cook constitutive model for the numerical simulation of metal cutting [4]. The literature seems also to show that model calibration for metal cutting simulation brings up some outstanding issues [5]. Severe plastic deformation through shear plane under high strain rates and temperatures tends to make the material characterization challenging. Because of this, inverse identification of the material parameters based on orthogonal machining tests carried out in advance is often used as an alternative approach for the calibration of constitutive models. But though inverse identification may allow a more efficient calibration from the viewpoint of the implementation effort, avoiding the costly and complexity of the experimental requirements, it is important to mention that obtained parameters include additional contributions not directly related to the plastic deformation (such as the tool geometry, friction,

fracture toughness, etc). In fact, some researches claimed that even although material parameters may be made to achieve a satisfactory correlation with the measured process parameters (such as the cutting force, shear angle, chip curling, etc), it is impossible to match all at the same time [6]. Consequently, there is an increased need for new easy-to-perform and low-cost mechanical testing methodology, to allow direct and fast identification of the material parameters and promote the predictive capability of numerical simulation models.

Compression of solid cylinders is often used to assess the material parameters for the constitutive models. This simple mechanical test (usually performed quasi-statically) is obviously not representative of the levels of strain-rate and temperature that are currently attained by industrial metal cutting operations. As a result of this, some alternative testing procedures have been proposed, with emphasis for experimental high speed equipment such as Taylor's impact tests or Hopkinson's compression and shear devices, among others. These devices can provide working conditions close to machining, but some of them are based on inverse analysis techniques while others need expensive experimental apparatus only available on a limited number of research laboratories. Depending on the chosen technique, it will have advantages but also disadvantages depending on how it is employed, especially lack of knowledge in how other parameters such as friction coefficient can affect the results. Considering these constraints several researchers have been working to improve testing methods, yet there is still plenty of scope for further development in this area [5].

The abovementioned difficulties to obtain the flow curves at appropriate rates of loading justify the following two-fold goal of this paper: (i) to propose an experimental methodology to estimate flow stress at the appropriate rates found in real metal cutting and (ii) to validate the referred methodology against direct measurements of the flow stress. The proposed low-cost testing methodology is intended to be easy-to-perform at any research laboratory since there are no special requirements. This proposal is based on traditional indentation hardness test that is a well-known and highly accepted methodology for mechanical characterization at quasi-static conditions. Here it is used to assess the so-called strain rate history effect [7, 8] which means that strain rate plays an important role on key microstructural features, such as grain refinement, accumulation, arrangement of dislocations and dynamic failure mechanisms [9, 10].

The overall presentation is supported by specially designed compression experiments that were performed on aluminium alloy AA1050 test specimens in a full annealed condition under laboratory-controlled conditions. The testing machine was designed and fabricated by the authors; constructive details are given for those readers that may be interested in developing a low-cost equipment for mechanical characterization at high rates of loading. The flow stress of the aluminium alloy AA1050 is estimated by using the yield stress from static Vickers hardness and the obtained results are compared with those from high strain rate testing. Another important consideration, which is not explicitly addressed in the manuscript but is implicit in the proposal, is that frictional contribution plays a central role, above and beyond

instantaneous flow stress rate-sensitivity. For that, a quick-stop device is also proposed which, will contribute towards further reducing frictional contribution on the plastic flow. Interrupted compression tests have allowed to clean and lubricate the contact interface for each incremental deformation. Real flow stress is expected to be much closer to yield stress at metastable conditions (after compression test) than to instantaneous flow stress under frictional influence (during compression test).

2. Experimental background

The material employed in the experimental tests was an aluminium alloy AA1050 (99.5% wt) with metallurgical properties resulting from annealing at 450ºC (2h followed by natural cooling in air). The initial grain size of the specimens after annealing were measured by metallographic examination and it was found to varies from 100 to 300μm. The stress–strain curves were obtained by means of compression tests carried out at room temperature on cylindrical specimens with 6mm diameter and 6mm height. The plan of experiments was designed in order to characterize the flow stress for a wide range of loading rates, and were carried out in a universal testing machine (quasi-static) and in a home-made equipment specifically intended for this research (high velocity).

The gas gun machine designed and implemented by the authors is schematically showed in Fig. 1. The main components can be divided into two main groups; (i) basic structural parts, and (ii) specific pneumatic and mechanical parts. No additional displacement monitorization or force sensors are required because of material strength and specimen deformation can be measured afterwards, and a more substantially compact design can be implemented. Basic structural parts comprise components such as the support table (bench), the guiding supports, and the pneumatic linear bearings, which are independent of the type of testing (e.g. monotonic or interrupted tests), operation conditions and materials to be characterized. These components are always to be used. Specific pneumatic and mechanical parts comprise those components such as the pressure vessel, the launcher tube, the striker bar, the quick-stop device (compression limiter) and the rubber dumper, whose design may be dependent on the type of testing, operation conditions and materials to be characterized. In general terms, currently installed compressed gas gun testing machine consist of two slender cylindrical bars of the same diameter, called the transmitter bar (motionless bar) and the striker bar (shorter cylindrical projectile). The compression plates used in the experimental tests have been machined and polished in order to limit surface roughness below $Ra < 0.1\mu m$. The control of asperity interlocking is important to promote uniform material expansion and homogeneous plastic deformation.

The striker bar is launched by a sudden release of the pressurized gas present in the pressure storage vessel and accelerates in a linear tubular guide until it impacts on the test specimen. The incident bar velocity is controlled by the gas pressure while the strain increment is limited by the quick-stop device (high strength metallic washer) defining the final height of the deformed specimen. Several configurations were used to evaluate the influence of the plastic strain on the material

hardness (washer thickness ranging from 1.5 to 5.5mm). However, it is clear that at these significantly high strain rate testing conditions the involved momentum and energies would be greatly enhanced by impact velocity. In fact, after the compression test, the remaining energy is high enough to damage the testing machine components. Thus, the striker bar weight has been properly adjusted during the experimental research. The velocity ranges from 2 to 60m/s corresponding to a striker bar weight ranging from 2Kg to 25g, respectively. Teflon sabot was used to assist the shorter striker bars while the movement is being performed. Furthermore, in order to reduce vibrations, propagation and reflection of elastic waves due to high velocity impact, a rubber damper is also used. Finally, after compression, the material strength is determined by micro hardness measurements using a Struers hardness tester model Duramin -1/-2 with a Vickers diamond, applying a load of 4.9N during a loading time of 15 seconds. The hardness measurements were performed in the specimen top. In order to verify this procedure, an additional three-dimensional mapping of the hardness has been performed along the radial and tangential direction of the specimens cross-section. The measurements showed a uniform distribution of the material hardness. Material strains are calculated by measuring the initial and final specimen lengths.
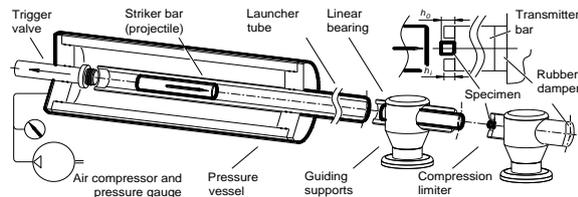
Fig. 1. Schematic representation of the pressured gas gun testing machine.

3. Results and discussion

3.1. Strain-rate effects on hardness

In order to show the influence of strain in the hardness of metallic materials, the hardness-strain curve of AA1050 was obtained by means of uniaxial compression tests performed under quasi-static conditions (that is, under very low values of strain-rate, $\dot{\varepsilon} \leq 10^{-2} s^{-1}$). The compression tests were performed for two different testing conditions (i) monotonic deformation and (ii) interrupted deformation. The interrupted compression tests were performed with specimens supplied by two different companies and the experiments consists on keeping a certain control of friction by maintaining a permanent lubrication of the contact interface between specimens and compression plates. Contact interfaces are cleaned and lubricated with oil after every incremental compression and the maximum strain increment was limited ($\varepsilon < 0.05$) to minimize friction contribution. The hardness of the deformed specimens is measured (i) after the compression tests for monotonic deformation conditions, and (ii) after each incremental deformation for interrupted tests.

Figure 2 shows the evolution of hardness with effective strain for the AA1050 in accordance with the experimental

methodology previously described. The logarithmic scale instead of the linear one has been used on the horizontal axis in order to facilitate reading of the results. As seen, the hardness measurements obtained with the monotonic tests (Monotonic in Fig. 2) are similar to those attained with interrupted tests (Interrupted in Fig. 2). Additionally, it should be noted that no significant differences between materials (from different suppliers) have been found indicating that these experimental results could be easily reproduced.

A simple graphic analysis of Fig. 2 allows the identification of three different regions: (a) a leftmost region ($\varepsilon < 0.04$), where the hardness is nearly constant and takes the smallest value at the origin, (b) a rightmost region ($\varepsilon > 2$), where the hardness seems to grow asymptotically and reaches the largest value among all the test cases, and (c) a region in between where the hardness value progressively grows from the smallest to the largest measured values. In the leftmost region, it is worth noticing that experimental data trend does not pass through the origin and the positive hardness interception is the material hardness measure of the full annealed AA1050. In fact, before work hardening, the lattice of the material exhibits a regular, nearly defect-free pattern. As the material is work hardened it becomes increasingly saturated with new dislocations storage and its arrangement in dislocation cells, and more dislocations are prevented from nucleating. Wherefore, there is more pronounced contributions related to misorientations between dislocation cells, and mainly between grains, that is associated with deformation stage IV. Additional hardness measurements have been done based on large strain testing techniques to estimate the maximum material hardness (please see 'Multi', $\varepsilon \cong 5$ and $\varepsilon \cong 10$, in Fig. 2). Then, the rightmost region of the graphics shows the typical large strain behaviour of deformation in FCC and BCC metals in which the annihilation process of dislocations promotes a constant material hardness [11]. Overall, there seems to be limited range between the full annealed condition of the AA1050 (asymptotically value of ~22HV) and the toughened and high strengthen material (asymptotically value of ~49HV) on hardness evolution under quasi-static kinematic conditions.
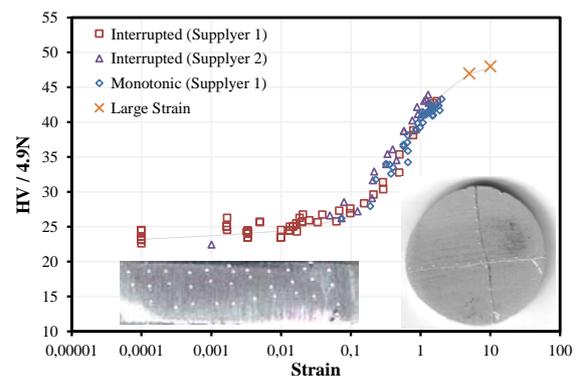
Fig. 2. Hardness-Strain data obtained from quasi static compression tests; Insets show measurements in top and cross-section of the specimens.

Figure 3 shows the experimental correlation between the yield stress and the corresponding material hardness for AA1050 in accordance with the experimental methodology

previously described. The graphical representation was performed for two different test conditions (i) monotonic deformation and (ii) interrupted deformation, based on the experimental data presented in Fig. 2. As seen, the stress-hardness relationship obtained in the monotonic deformation (Monotonic in Fig. 3) are similar to those obtained with interrupted tests (Interrupted in Fig. 3). Nevertheless, a more attentive look reveals a slight stress divergence with increasing hardness which is believed to be due friction effects.

There are many valiant analytical correlations between the yield stress and material hardness, particularly under quasi-static kinematic conditions [12]. However, in what follows experimental data in Fig. 3 has been used in order to illustrate the adopted approach. For this purpose, Eq. 1 presents a correlation between the current material hardness (HV) and the yield stress (σ_y), where c_0 and c_1 are constants to be determined from experimental results considering hardness-strain and stress-strain data. It is noticeable from Fig. 3 that both evolutions can be well adjusted by a linear regression. Other authors also found similar trends to our findings [13].

Calibration of Eq. 1 considering experimental data of Fig. 2 for aluminum AA1050 under quasi static conditions at room temperature results in the following constants: (i) $c_0 = 5.83$ and $c_1 = 78.35$ for monotonic deformation, and $c_0 = 5.09$ and $c_1 = 58.68$ for interrupted deformation.
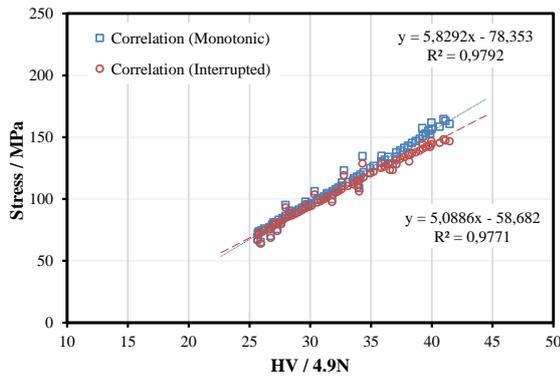
Fig. 3. Experimental correlation between yield stress and material hardness.

Figure 4 shows the evolution of hardness with effective strain for AA105 performed at quasi-static conditions ($\dot{\varepsilon} \sim 10^{-2} s^{-1}$) and high velocity compressions performed at constant strain-rates of $2 \cdot 10^3$, $4 \cdot 10^3$ and $1.1 \cdot 10^4 s^{-1}$. By analyzing the results presented in Fig. 4, it should be noted the influence of imposed strain-rate on the material hardness evolution. This rate-dependence occurs in a manner that, for a given strain level, current material hardness increases with strain-rate. In an intermedium strain level, in which plastic deformation is already considerable ($\varepsilon > 0.2$) and strain-hardening is yet substantial (in the region $\varepsilon < 1$), a maximum of the rate-dependence is observed. This result is in line with the findings of the graphic analysis of Fig. 2 where material hardness seems also to reach an asymptotic hardness of 49HV, although at a much slower rate than at high strain rate conditions.

At the most aggregate level, constitutive models should be also able to reproduce sufficiently well the material hardness

from the beginning when a compression specimen starts to deform until it reaches severe plastic deformation at high strain-rates. Its physical principle is based on the fact that both hardness and yield stress are material strength parameters, evidencing a linear correlation of the experimental data. The hardness-strain curves were fitted by the simplified Johnson-Cook (Eq. 2) and the Silva empirical expression (Eq. 3) [14], where the *A*, *B*, *C*, *D*, *m* and *n* are constants to be determined from experimental data. It should also be noted that Eq. 3 can be transformed into Eq. 2 when D_{SH}, $m_{SH} = 0$ (subscript *H* refers to hardness). In addition, Silva model can be also simplified this way into the Ludwik-Holloman equation and into the Voce equation when D_{SH}, m_{SH}, $C_{SH} = 0$ and D_{SH}, n_{SH}, $C_{SH} = 0$, respectively.
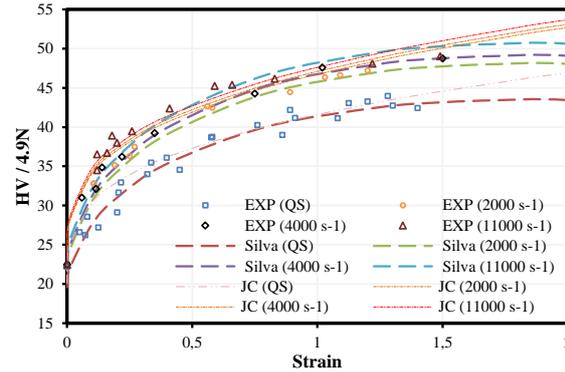
Fig. 4. Hardness-strain data obtained from constant high strain-rate tests.

Calibration of Eq. 2 and Eq. 3 considering experimental data of Fig. 4 results in the following material constants $A_{JH} = 0.88$ MPa, $B_{JH} = 22.75$ MPa, $C_{JH} = 0.28$ and $n_{JH} = 0.31$ for the Johnson-Cook model and $A_{SH} = 0.67$ MPa, $B_{SH} = 24.41$ MPa, $C_{SH} = 1.04$ MPa, $D_{SH} = 106.01$, $m_{SH} = -0.29$ and $n_{SH} = -0.29$ for the Silva model. These parameters were determined using an optimization routine to provide the best fit to the experimental data (software Datafit). The flow curves resulting from this calibration procedure are plotted in Fig. 4 and indicate that major differences are due to material strength saturation at high strain. Unfortunately, commonly used Johnson-Cook´s simplified models are often limited to a 'positive' hardening where the material strength increase continuously. The Silva model (Eq. 3) has the special ability for displaying material strength saturation at high values of strain; Thus, this mathematical equation seems therefore appropriate to describe the hardness evolution and it is general enough to permit fitting flow softening if required for material behaviour modelling.

$$\sigma_y + A_P = c_0 + c_1 \cdot H_V \tag{1}$$

$$\sigma = \left(A_{JH} + \varepsilon^{n_{JH}}\right)\left(B_{JH} + \ln \dot{\varepsilon}^{C_{JH}}\right) \tag{2}$$

$$\sigma = \left(A_{SH} + e^{m_{SH}\varepsilon}\varepsilon^{n_{SH}}\right)\left(B_{SH} + C_{SH} \ln\left[D_{SH} + \dot{\varepsilon}\right]\right) \tag{3}$$

3.2. Strain-rate effects on flow stress

In order to show the influence of strain-rate in the mechanical response of AA1050, the stress-strain curves were obtained by means of uniaxial compression tests performed under (i) quasi-static conditions on a conventional CNC

hydraulic press and (ii) high strain-rate conditions on an electromagnetic cam apparatus (fully instrumented) [14]. The experimental data resulting from the tests is depicted in Fig. 5. Results show the combined influence of strain and strain-rate in the overall stress response, and indicate that AA1050 presents significant strain-rate sensitivity. The 'saw tooth' oscillations is attributed to the dynamic testing conditions. The flow stress-strain curves were fitted by following the procedure described in previous section (subscript H is changed to Y, referring yield stress), where the new material constants are A_{JY} = 0.38 MPa, B_{JY} = 117.9 MPa, C_{JY} = 2.5 and n_{JY} = 0.42 for the Johnson-Cook model and A_{SY} = 0.41 MPa, B_{SY} = 45.8 MPa, C_{SY} = 12.3 MPa, D_{SY} = 367.8 , m_{SY} = -0.08 and n_{SY} = 0.50 for the Silva model. Both empirical models show now good agreement with experimental data, mainly because there is not an asymptotic value in the experimental data.
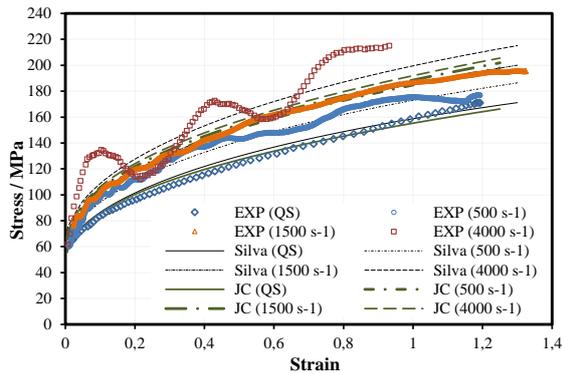
Fig. 5. Stress-strain data obtained from high strain-rate tests.

Additional tests, concerning stress-strain curve were obtained by means of compression tests performed at (i) monotonic deformation, and (ii) interrupted deformation. The experimental data resulting from the tests is depicted in Fig. 6 and it is possible to notice a good agreement amongst these particular testing conditions until a relative large strain of $\varepsilon \sim 0.5$. As the plastic deformation develops, a progressive divergence in the flow stress response starts to emerge. This difference between the monotonic and interrupted deformation is due to an extra frictional contribution at severe plastic deformation. Contact interface area between material specimen and compression plates rises significantly as the contact pressure increases, thereby hampering the material flow and promote flow stress. This result is a macroscopic evidence of friction influence on the mechanical characterization of material that can be further modelled and used to correct experimental flow stress curves. The growing difference in the flow stress ($\Delta\sigma$) is shown in Fig. 6 (please see 'Friction') and can be fitted by an exponential curve as a function of effective strain (Eq. 4), where the A_F and n_F are constants to be determined from experimental data; the constant values are 1.27 and 2.35, respectively. Consequently, whenever such a monotonic deformation conditions are used, this experimental procedure should be applied to reduce the non-plasticity phenomena contributions in the stress-strain curve.

$$\Delta\sigma = A_F + e^{n_F \cdot \varepsilon} \qquad (4)$$

3.3. Flow stress estimation on basis of material hardness

The proposed methodology is based on the combined use of interrupted compression tests, considering constant strain-rate, and measurements of the material hardness after every incremental deformation. The instantaneous flow stress can be determined by the experimental correlation between the yield stress and corresponding material hardness. Then, having Eq. 1 and calibration parameters for interrupted deformation tests (given in section 3.1), the rate-dependent yield stress can be estimated from rate-dependent hardness data presented in Fig. 4. For clarity purposes, it was used only Eq. 3 as it is the one which is able to simultaneously address issues related to yield stress and flow stress. Obtained calculation are showed in Fig. 7 performed at quasi-static conditions ($\dot{\varepsilon} \sim 10^{-2} s^{-1}$), and high velocity compressions performed at constant strain-rates of $5 \cdot 10^2$, $1.5 \cdot 10^3$ and $4 \cdot 10^3 s^{-1}$ (Hardness in Fig. 7).
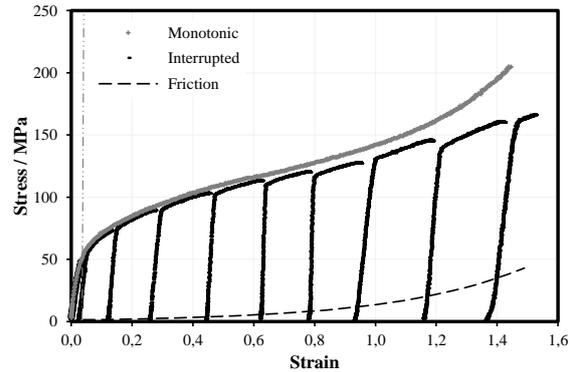
Fig. 6. Stress-strain data obtained from monotonic and interrupted tests.

In order to evaluate whether the proposed methodology is suitable for estimate the instantaneous material response, the calculated estimates for the flow stress based on material hardness were compared with the experimental measures of the flow stress. But firstly, there is the need to minimize frictional contribution that is significant in severe monotonic deformation conditions. All monotonic tests suffer from over-estimating the instantaneous flow stress (e.g. split Hopkinson bar test). Experimental data in Fig. 5 have been subsequently processed, having Eq. 4 and calibration parameters for interrupted deformation tests (given in section 3.2), and presented in Fig. 7 (please see 'Silva (corrected)').

Results show good agreement between the calculated estimates and the post-processed experimental data of the flow stress for the tested strain-rate range. These results show that flow stress can be successfully estimated by the proposed methodology avoiding expensive and complex experimental apparatus (load dynamometers, displacement transducers, high definition video, data acquisition systems, etc). Additionally, interrupted tests allow to reduce sliding friction and, this way, minimizing unwanted energy contribution to the flow stress curve.
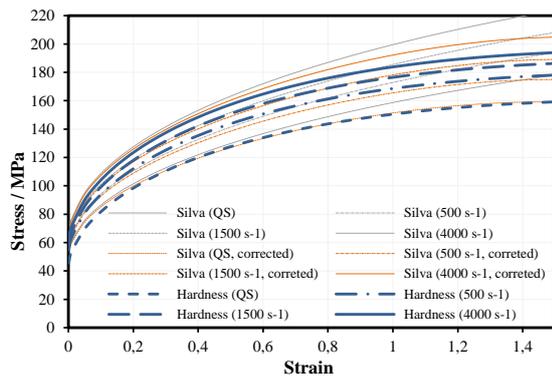
Fig. 7. Flow stress estimation based on material hardness after impact tests.

4. Conclusions

This paper presents a simplified methodology for the mechanical characterization of materials under high rates of loading without investing in expensive hardware and software. Here, stress relaxation related to viscous mechanisms is considered as a minor contribution to the yield stress and therefore material hardness could be deemed as a measure of the instantaneous flow stress. A relatively low-cost testing equipment with a quick-stop device was therefore planned and built to provide a suitable equipment to assess the proposed methodology. The effective strain and yield stress have been measured after completion of the test and, consequently, expensive instrumentation and high speed data acquisition systems were not necessary.

Results shown the adequacy of the testing machine operating both for monotonic and interrupted compression to successfully perform the mechanical characterization of materials under high impact rates of loading. A traditional high speed testing has been used for validation purpose. However, it is important to note that the material parameters can be determined exclusively by the proposed easy-to-perform and low-cost methodology stress based on material hardness.

Results also shown that incremental testing conditions are able to minimize friction contribution in the experimental force records caused by inadequate lubrication conditions. This takes greater significance for severe monotonic deformation, because contact phenomena become even more prominent than viscous effects. Thus, an even more accurate yield stress measurement can be obtained with compressions tests using interrupted deformation. However, the principal outcome is related to the validation of the proposed methodology to estimate flow stress based on material hardness. Experimental data has demonstrated that strain-rate has a significant influence on the material microstructure and that materials hardness may accurately be used to estimate flow stress under high rates of loading.

The proposed technique seems also to be adequate for very high strain-rate testing. The variation of force with displacement obtained from the traditional experimental tests

above 10^3 s^{-1} is often difficult to process due 'saw tooth' oscillations that are observed at the early stages of the deformation. This is attributed to the dynamic testing conditions (inertia forces and stress wave propagation under high impact loading) that disturb the results analysis. This is even more problematic when the compression test needs to run above 10^4 s^{-1} when sensors begin to fail. The proposed methodology does not suffer this disadvantage and can therefore deform with preselected values at very high strain rate. The application of this methodology to very high strain rate conditions could provide a new level of understanding about the mechanical characterization of materials for metal cutting.

References

[1] Zerilli FJ, Armstrong RW. Dislocation-mechanics based constitutive relations for material dynamics calculations. J Appl Phys 1987; 6 (5): 1816-1825.
[2] Gao C, Zhang L. Constitutive modelling of plasticity of fcc metals under extremely high strain rates. Int J Plasticity 2012; 32: 121-133.
[3] Santos T, Rosa PAR, Maghous S, Rossi R. A simplified approach to high strain rate effects in cold deformation of polycrystalline FCC metals: Constitutive formulation model calibration. J Plasticity 2016; 82: 76-96.
[4] Özel T, Altan T. Determination of Workpiece flow stress and friction at the chip-tool contact for high-speed cutting. Int J Mach. Tools & Manuf. 2000;40: 133-152.
[5] Arrazola PJ, Özel T, Umbrello D, Davies M, Jawahir IS. Recent advances in modelling of metal machining processes. CIRP Ann. Technol. 2013; 62:695-718.
[6] Bil H, Kiliç SE, Tekkaya AE. A comparison of orthogonal cutting data from experiments with three different finite element models. Int. J. Mach. Tools & Manuf. 2004; 44: 933-944.
[7] Klepaczko J. Thermally activated flow and strain rate history effects for some polycrystalline f.c.c. metals. Materials Science and Engineering 1975: 18: 121-135.
[8] Tanner AB, McGinty R D, McDowell DL. Modeling temperature and strain rate history effects in OFHC Cu. Int J Plasticity1999;15: 575-603.
[9] Huang F, Tao N. Effects of strain rate and deformation temperature on microstructures and hardness in plastically deformed pure aluminum. J Materials Science & Technology 2011; 27: 1-7.
[10] Dolinski M, Rittel D, Dorogoy A. Modeling adiabatic shear failure from energy considerations. J Mech. Physics of Solids 2010; 58: 1759-1775.
[11] Les P, Stuewe HP, Zehetbauer M. Hardening and strain rate sensitivity in stage IV of deformation in f.c.c. and b.c.c. metals. Materials Science and Engineering: A 1997; 234: 453-455.
[12] Johnson K. The correlation of indentation experiments. J Mechanics and Physics of Solids 1970; 18: 115-126.
[13] Tiryakioglu M, Robinson J, Salazar-Guapuriche M, Zhao Y, Eason P. Hardness-strength relationships in the aluminum alloy 7010. Materials Science and Engineering: A 2015; 631: 196-200.
[14] Silva CMA, Rosa PAR, Martins PAF. Electromagnetic Cam Driven Compression Testing Equipment. Experimental Mechanics, Experimental Mechanics 2012; 52: 1211-1222.